Energy Conversion and Management 86 (2014) 388–398

Contents lists available at ScienceDirect

Energy Conversion and Management

journal homepage: www.elsevier.com/locate/enconman

A comprehensive measure of the energy resource: Wind power potential (WPP)

Jie Zhang [a,*], Souma Chowdhury [b], Achille Messac [c]

[a] National Renewable Energy Laboratory, Golden, CO 80401, USA
[b] Department of Mechanical Engineering, Mississippi State University, Mississippi State, MS 39762, USA
[c] Department of Aerospace Engineering, Mississippi State University, Mississippi State, MS 39762, USA

ARTICLE INFO

Article history:
Received 20 February 2014
Accepted 25 April 2014

Keywords:
Anisotropic lognormal distribution
Farm siting
Layout optimization
Response surface
Wind power density
Wind resource assessment

ABSTRACT

Currently, the quality of available wind energy at a site is assessed using wind power density (WPD). This paper proposes to use a more comprehensive metric: the wind power potential (WPP). While the former accounts for only wind speed information, the latter exploits the joint distribution of wind speed and wind direction and yields more credible estimates. The WPP investigates the effect of wind velocity distribution on the optimal net power generation of a farm. A joint distribution of wind speed and direction is used to characterize the stochastic variation of wind conditions. Two joint distribution methods are adopted in this paper: bivariate normal distribution and anisotropic lognormal method. The net power generation for a particular farmland size and installed capacity is maximized for different distributions of wind speed and wind direction, using the Unrestricted Wind Farm Layout Optimization (UWFLO) framework. A response surface is constructed to represent the computed maximum wind farm capacity factor as a function of the parameters of the wind distribution. Two different response surface methods are adopted in this paper: (i) the adaptive hybrid functions (AHF), and (ii) the quadratic response surface method (QRSM). Toward this end, for any farm site, we can (i) estimate the parameters of the joint distribution using recorded wind data (for bivariate normal or anisotropic lognormal distributions) and (ii) predict the maximum capacity factor for a specified farm size and capacity using this response surface. The WPP metric is illustrated using recorded wind data at four differing stations in the state of North Dakota. The results illustrate the variation of wind conditions and, subsequently, its influence on the quality of wind resources. A comparison of four sites in North Dakota shows that WPD and WPP follow different trends, and the ranking of candidate sites in terms of a realistic resource potential measure is not captured by WPD.

1. Introduction

In recent years, social and scientific needs have been concerned with the carbon footprint in the atmosphere as well as the dependence on oil masses. Investing in wind energy, a viable source of energy, is becoming increasingly important. Planning an appropriate location for a wind farm (farm siting) is crucial to the performance and economy of the farm. The available wind resource, distance to power grid connections, local topography, access to transportation, wind variability, cost of energy (COE), and likely environmental impact are the major factors that need to be considered in wind farm siting. In the case of offshore wind, COE becomes a critical concern to achieve desired goals set by the U.S. Department of Energy. Because of the highly stochastic nature of wind, the distribution of the potential wind resources and prediction of the optimal power generation capability of a farm at that site remain challenging tasks.

Wind power density (WPD) is a useful way to evaluate the available wind resource at a potential site. WPD, measured in watts per square meter, indicates how much energy is available at the site. WPD (W/m^2) is a nonlinear function of the probability density function (*pdf*) of wind speed, which is expressed as [1]

$$WPD = \frac{1}{2}\rho \int_0^{U_{max}} U^3 f(U) dU \quad (1)$$

where U represents the wind speed; U_{max} is the maximum possible wind speed at that location; ρ represent the air density; and $f(U)$ is the *pdf* of the wind speed.

* Corresponding author. Tel.: +1 303 275 4428.
E-mail address: jie.zhang@nrel.gov (J. Zhang).

http://dx.doi.org/10.1016/j.enconman.2014.04.083
0196-8904/

The wind resource varies significantly from one location to another. Landberg et al. [2] presented an overview of the different ways to estimate the wind resources at a site. The paper showed that the increasingly widespread utilization of wind energy and different terrain types throughout the world presented a number of challenges to classical wind resource estimation. Celik [3] studied wind energy potential based on the Weibull and Rayleigh models and found that the Weibull model provided better power density estimations than the Rayleigh model in all 12 months. Celik [4] also concluded that the final judgement of the suitability of a possible wind speed distribution function must be based on the standard deviation of the WPD. Velo et al. [5] proposed a neural networks-based method to determine the annual average wind speed at a complex terrain site based on short-term wind data. In addition, a significant amount work has been done to assess the wind potential at specific locations [6–11]. Lu et al. [6] estimated the potential for electricity generation on Hong Kong islands through an analysis of the monthly wind speed probability density and WPD (for different ground levels). Karsli and Geçit [7] presented a preliminary examination of the wind potential of the Nurdagı-Gaziantep district in Turkey by estimating the WPD based on Weibull wind speed distribution. Rehman [8] analyzed the annual, seasonal, and diurnal variations of long term wind data at Yanbo which is located on the west coast of Saudi Arabia. Boudia et al. [9] analyzed the wind characteristics of four locations in Algerian Sahara using Webull distribution. Tizpar et al. [10] also used Weibull distribution to evaluate the wind potential of Mil-E Nader region in Sistan and Baluchestan Province, Iran. The wind resource of selected locations along the coastal region of Ghana was evaluated by Adaramola et al. [11].

1.1. Motivation and objectives

WPD is the prevailing measure of wind resource potential at a site, but it accounts for only wind speed. To estimate energy potential, factors impacting maximum power generation and the COE of a farm also include the (i) distribution of wind direction, (ii) layout of the wind farm, and (iii) appropriate turbine type selection. Thereby, these factors are critical for determining the quality of a wind energy site and designing an optimum wind farm configuration on that site. Therefore, one of the objectives in this paper is to investigate the effect of wind distribution and optimal farm layout on the wind resource potential at a site.

An optimal layout of turbines that ensures maximum farm efficiency is of utmost importance in conceiving a wind farm project and in making wind a competent source of energy [12]. For a given farm layout, the direction of wind has a strong influence on the wakes created (i.e., the shading effect of a wind turbine on other turbines downstream from it) and subsequently on the overall flow pattern in a wind farm. Therefore, the direction of wind plays an important role in evaluating the quality of wind resources (wind energy potential) at a farm site.

In the literature, WPD has been used to estimate the available wind power for a single turbine. It would be useful if we could estimate the power generated by a wind farm by considering the joint distribution of wind speed and direction. In addition, it would be uniquely helpful if we could estimate the maximum power generated by a wind farm with optimum farm layout. Toward this end, this paper develops a more comprehensive method to characterize and predict the quality of wind resources at a site. We propose to use a more comprehensive metric: the wind power potential (WPP). The WPP accounts for the joint distribution of wind speed and wind direction, which yields more credible estimates. The remainder of the paper is organized as follows. The WPP metric is developed in Section 2. Section 3 presents two numerical examples that illustrate the use of the WPP metric. Concluding remarks and future work are given in the last section.

2. The wind power potential (WPP) model

In this paper, the WPP model makes significant assumptions and approximations in modeling the optimal wind farm power generation, including: (i) a fixed farm orientation (biased toward certain wind directions) is used, and (ii) a particular turbine type (biased toward certain wind speeds) is used. The WPP model is developed to evaluate the wind power potential (maximum wind farm capacity factor for a specified farm size and installed capacity) for differing locations by observing the following sequence of four steps.

- **STEP 1**: Using recorded wind data at a location, the joint distribution of wind speed and direction is estimated to characterize the wind conditions. In this paper, two types of distributions are adopted: (i) bivariate normal distribution [13] and (ii) anisotropic lognormal distribution. The parameters of bivariate normal distribution include five variables: (i) the mean of the wind speed distribution, μ_U; (ii) the mean of the wind direction distribution, μ_θ; (iii) the variance of the wind speed distribution, σ_U; (iv) the variance of the wind direction distribution, σ_θ; and (v) the correlation coefficient between wind speed and wind direction, ρ. The anisotropic lognormal distribution also has five parameters: (i) the prevailing wind direction, θ_D; (ii) the mean of the lognormal lateral wind speed distribution, $\mu_{x'}$; (iii) the standard deviation of the lognormal lateral wind speed distribution, $\sigma_{x'}$; (iv) the mean of the lognormal longitudinal wind speed distribution, $\mu_{y'}$; and (v) the standard deviation of the lognormal longitudinal wind speed distribution, $\sigma_{y'}$. Every unique combination of these five parameters represents a unique sample distribution of wind speed and wind direction.
- **STEP 2**: The five parameters of the bivariate normal distribution (or the anisotropic lognormal distribution) are sampled using design of experiment (DoE) methods. The Sobol's quasirandom sequence generator [14] is adopted in this paper.
- **STEP 3**: For each sample distribution of wind speed and wind direction, we maximize the net power generation through farm layout optimization. Toward this end, we employ the Unrestricted Wind Farm Layout Optimization (UWFLO) methodology [12].
- **STEP 4**: A response surface is constructed to represent the computed maximum capacity factor as a function of the parameters of the bivariate normal distribution (or the anisotropic lognormal distribution). Two response surface methods are adopted for this purpose: (i) the adaptive hybrid functions (AHF) [15], and (ii) the quadratic response surface method (QRSM) [16].

For any farm site, according to the recorded wind data, we can (i) estimate the parameters of the joint distribution of wind speed and direction (bivariate normal or anisotropic lognormal) and (ii) predict the maximum capacity factor for a specified farm size and capacity by using the WPP model. Fig. 1 illustrates the overall structure of the WPP model. In the subsequent sections, we discuss the details of each step.

2.1. Distribution of wind speed and wind direction

The power generated by turbine-j (P_j) for an incoming wind speed U_j is given by

$$P_j = k_g k_b C_p \left(\frac{1}{2}\rho_a \pi \frac{D_j^2}{4} U_j^3\right) \tag{2}$$

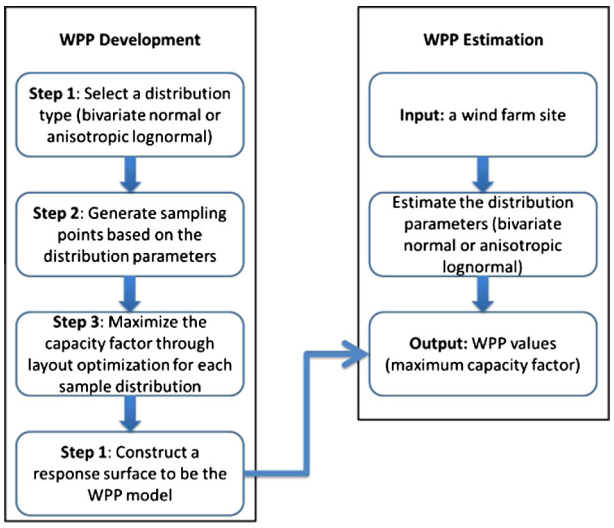

Fig. 1. Overall structure of the WPP model.

where C_p, k_b, and k_g are the power coefficient, the mechanical and the electrical efficiencies of the turbine, respectively; and ρ_a represents the density of air.

The net power generated, P_{farm}, is given by

$$P_{farm} = \sum_{j=1}^{N} P_j \tag{3}$$

where P_j represents the power generated by Turbine-j; N is the number the turbines in the farm.

The power generated by an individual turbine is a cubic function of the approaching wind speed (as shown in Eq. (2)). On the other hand, the wind direction, together with the farm layout, are two major factors that regulate the overall flow pattern (wake patterns) inside the wind farm. The determination (or prediction) of the annual power generation from a wind farm should thereby account for the variations in both wind speed and wind direction. This prediction is accomplished using the following two-step procedure:

1. Estimate the annual joint distribution of the wind speed and wind direction (as a *pdf*).
2. Integrate the power generation model (for a given wind speed/and direction) throughout the entire annual wind distribution.

A variety of joint distributions of wind speed and wind direction are available in the literature. Vega and Letchford [17] used the Weibull distribution to estimate the wind speed probability and took the shape parameter and the scale parameter as functions of wind direction. Carta et al. [18] presented a joint probability density function of wind speed and wind direction for wind energy analysis. Erdem and Shi [19] compared three bivariate joint distributions (angular–linear, Farlie–Gumbel–Morgenstern, and anisotropic lognormal approaches) for wind speed and wind direction data.

In this paper, two types of joint distributions are adopted—(i) bivariate normal distribution and (ii) anisotropic lognormal distribution—to simultaneously characterize the variation of wind speed and wind direction.

2.1.1. Bivariate normal distribution

The variation of both the wind speed and the wind direction need not follow a bivariate normal distribution. However, in this paper we represent the wind resource potential of a wind site as a function of the parameters of the wind distribution. The bivariate normal distribution presents only five parameters, which allows a tractable approach to our objective. Other more accurate distributions are likely to present an appreciably large set of parameters; in that case, the subsequent parametric determination of the wind resource potential (through sampling and optimization) would become practically prohibitive. The *pdf* of bivariate normal distribution is expressed as

$$p(U,\theta) = \frac{1}{2\pi\sigma_U\sigma_\theta\sqrt{1-\rho^2}} \exp\left[-\frac{z}{2(1-\rho^2)}\right] \tag{4}$$

where,

$$z \equiv \frac{(U-\mu_U)^2}{\sigma_U^2} - \frac{2\rho(U-\mu_U)(\theta-\mu_\theta)}{\sigma_U\sigma_\theta} + \frac{(\theta-\mu_\theta)^2}{\sigma_\theta^2} \tag{5}$$

where U and θ represent the wind speed and wind direction, respectively; μ_U and μ_θ are the means of the wind speed distribution and the wind direction distribution, respectively; σ_U and σ_θ represent the variances of the wind speed distribution and the wind direction distribution, respectively; and ρ is the correlation coefficient between the wind speed and wind direction distributions. The parameters of the distribution are estimated using the *maximum likelihood* method.

It is important to note that the bivariate normal distribution may not accurately characterize the joint distribution of wind speed and wind direction in some siting locations. However, the objective of this paper is not to develop an accurate distribution of wind speed and wind direction, but to evaluate the energy resource potential at a site. The main concern in this paper is to capture the differences in wind distribution among siting locations, thereby to develop a response surface representing the computed maximum capacity factor as a function of the parameters of the wind distribution. Toward this end, the bivariate normal distribution can successfully capture the differences in wind distribution among different farm sites.

2.1.2. Anisotropic lognormal approach

The anisotropic lognormal approach was developed by Erdem and Shi [19] and adopts the concept of the anisotropic Gaussian model proposed by Weber [20]. Fig. 2 illustrates the prevailing wind direction and the axes. The parameter θ_D represents the angle between the prevailing direction and the North direction; the parameter θ indicates the angle between a wind direction and

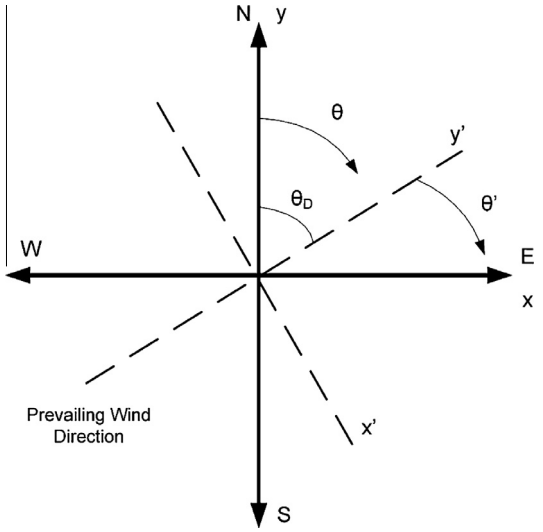

Fig. 2. Prevailing wind direction [19].

the North direction; the parameter θ' indicates the angle between a wind direction and the prevailing direction. The axes x' and y' represent the lateral and longitudinal axes with respect to the prevailing wind direction, respectively.

The joint distribution of wind speed and direction can be expressed in Eq. (6).

$$f(U,\theta')=\frac{1}{(U\sin\theta'-\gamma_{x'})(U\cos\theta'-\gamma_{y'})\sigma_{x'}\sigma_{y'}2\pi} \times\exp\left\{-\frac{\left[\ln(U\sin\theta'-\gamma_{x'})-\mu_{x'}\right]^2}{2\sigma_{x'}^2}-\frac{\left[\ln(U\cos\theta'-\gamma_{y'})-\mu_{y'}\right]^2}{2\sigma_{y'}^2}\right\} \tag{6}$$

where $\mu_{x'}$ is the mean of lognormal lateral wind speed distribution; $\sigma_{x'}$ is the standard deviation of the lognormal lateral wind speed distribution; $\gamma_{x'}$ is the location parameter of the lognormal lateral wind speed distribution; $\mu_{y'}$ is the mean of lognormal longitudinal wind speed distribution; $\sigma_{y'}$ is the standard deviation of the lognormal longitudinal wind speed distribution; and $\gamma_{y'}$ denotes the location parameter of the lognormal longitudinal wind speed distribution.

The joint distribution of wind speed and direction might be multimodel, which is shown in the paper by Zhang et al. [21,22]. Thus, it is possible that there are multiple prevailing directions. In that case, we can find all prevailing directions by dividing the entire wind direction spectrum into several sectors. In this paper, to restrict the number of the joint distribution parameters, we assume a single prevailing wind direction for the entire spectrum.

In the anisotropic lognormal approach, the prevailing wind direction (θ_D) can be determined using the following equation [19].

$$\theta_D=\begin{cases}\arctan\left(\frac{\bar{s}}{\bar{c}}\right); & \text{if } \bar{s}\geqslant 0,\bar{c}>0\\ \frac{\pi}{2}; & \text{if } \bar{s}>0,\ \bar{c}=0\\ \pi+\arctan\left(\frac{\bar{s}}{\bar{c}}\right); & \text{if } \bar{c}<0\\ \pi; & \text{if } \bar{s}=0,\bar{c}=-1\\ 2\pi+\arctan\left(\frac{\bar{s}}{\bar{c}}\right); & \text{if } \bar{s}<0,\bar{c}>0\\ \frac{3\pi}{2}; & \text{if } \bar{s}<0,\bar{c}=0\end{cases} \tag{7}$$

where $\bar{s}=\frac{1}{n}\sum_{i=1}^{n}U_i\sin\theta_i$ and $\bar{c}=\frac{1}{n}\sum_{i=1}^{n}U_i\cos\theta_i$; n is the number of recorded wind samples; U_i represents the i^{th} wind speed; and θ_i represents the angle between the i^{th} wind direction and the North direction.

2.1.3. Estimating the annual energy production

The total annual energy produced by a wind farm (in kWh), E_{farm}, at a particular location can be expressed as

$$E_{farm}=8760\int_{0^\circ}^{360^\circ}\int_{0}^{U^{max}}P_{farm}(U,\theta)p(U,\theta)dUd\theta \tag{8}$$

where, U^{max} is the maximum possible wind speed at that location, and $P_{farm}(U,\theta)$ represents the power generated by the farm for a wind speed U and a wind direction θ. In Eq. (8), $p(U,\theta)$ represents the probability of occurrence of wind conditions defined by speed U and direction θ. The power generated by the entire wind farm is a complex function of the incoming wind properties, the layout of turbines, and the turbine features. Hence, a numerical integration approach [23] is suitable for estimating the annual energy production as given by Eq. (8).

In this paper, we integrate the Monte Carlo method that is implemented through the Sobol's quasirandom sequence generator. This class of integration method is easy to apply (for multidimensional integrals) and likely to provide greater accuracy for the same number of function evaluations (at sample points) when compared to the repeated integrations using one-dimensional methods (deterministic quadrature rule methods). The approximated total annual energy produced by the wind farm is then expressed as

$$E_{farm}=\sum_{i=1}^{N_p}P_{farm}\left(U^i,\theta^i\right)p\left(U^i,\theta^i\right)\Delta U\Delta\theta \tag{9}$$

where

$$\Delta U\Delta\theta=U_{max}\times 360^\circ/N_p$$

where N_p is the number of sample points used; and the parameters U^i and θ^i, respectively, represent the speed and direction of the incoming wind for the i^{th} sample point. Hence, the annual energy is readily determined by the summation of the estimated power generation (P_{farm}) over a set of randomly distributed N_p wind velocities.

2.2. Parameter sampling

In problems with simulated data (such as the power generation form UWFLO), the choice of an appropriate sampling technique is generally considered crucial for the performance of any response surface approach. In this paper, the parameters of the joint distribution of wind speed and direction are sampled using the Sobol's quasirandom sequence generator [14]. Sobol sequences use a base of two to form successively finer uniform partitions of the unit interval, and then reorder the coordinates in each dimension. The algorithm for generating Sobol sequences is explained in Bratley and Fox, Algorithm 659 [24].

To develop the response surface to represent the computed maximum capacity factor as a function of the parameters of the wind velocity distribution, 100 sets of sample points (of wind velocity distribution) are generated as training and test points. For each sample set of distribution parameter, we maximize the net power generation using the UWFLO framework. The farm size and the installed capacity are fixed for all distributions. For the bivariate normal distribution, the sampling ranges are defined as follows according to numerical experiments: (*i*) $1\text{ m/s}<\mu_U<15\text{ m/s}$ at 3 m height; (*ii*) $0^\circ<\mu_\theta<360^\circ$; (*iii*) $0.5<\sigma_U<4$; (*iv*) $11.25<\sigma_\theta<90$; and (*v*) $0<\rho<1$. For the anisotropic lognormal distribution, the sampling ranges are defined as follows: (*i*) $-15\text{ m/s}<\mu_{x'}<15\text{ m/s}$ at 3 m height; (*ii*) $1<\sigma_{x'}<8$; (*iii*) $-15\text{ m/s}<\mu_{y'}<15\text{ m/s}$ at 3 m height; (*iv*) $1<\sigma_{y'}<8$; and (*v*) $0^\circ<\theta_D<360^\circ$.

2.3. Unrestricted Wind Farm Layout Optimization (UWFLO) methodology

The UWFLO methodology introduced by Chowdhury et al. [12,25] avoids the limiting assumptions presented by other methods, regarding the layout pattern and the selection of turbines. In the UWFLO method, the turbine location coordinates are treated as continuous variables, which allows all feasible arrangements of the turbines. The UWFLO method is applicable to both experimental-scale wind farms and full-scale commercial wind farms by

1. Using the wake growth model proposed by Frandsen et al. [26].
2. Implementing the wake superposition model developed by Katic et al. [27].
3. Including the estimated joint distribution of the wind speed and wind direction.
4. Modifying the power generation model to allow turbines with different hub heights and performance characteristics.
5. Evaluating the cost of the wind farm using an accurate response surface-based wind farm cost model (RS-WFC) [28].
6. Implementing a newly developed mixed-discrete particle swarm optimization (MDPSO) algorithm [29,30].

The overall optimization problem is defined as

$$\begin{aligned} \text{Max} \quad & f(V) = \frac{P_{farm}}{NP_{r0}} \\ \text{subject to} \quad & g_1(V) \leqslant 0 \\ & g_2(V) \leqslant 0 \\ & V = \{X_1, X_2, \ldots\ldots, X_N, Y_1, Y_2, \ldots\ldots, Y_N\} \\ & 0 \leqslant X_i \leqslant X_{farm} \\ & 0 \leqslant Y_i \leqslant Y_{farm} \end{aligned} \tag{10}$$

where P_{r0} is the rated power of the reference turbine (used for normalizing); P_{farm} is the power generated by the farm; and $f(V)$ represents the capacity factor. X_i and Y_i are the coordinates of the wind turbines in the farm. The parameters X_{farm} and Y_{farm} represent the extent of the rectangular wind farm in the X and Y directions, respectively. The inequality constraint g_1 represents the minimum clearance required between any two turbines. To ensure that the wind turbines are placed within the fixed-size wind farm, the X_i and Y_i bounds are reformulated into an inequality constraint, $g_2(V) \leqslant 0$.

2.4. Response surface development

In the literature [31,32], we can find a variety of response surface techniques that include: (i) QRSM, (ii) Kriging, (iii) radial basis functions (RBF), (iv) extended radial basis functions (E-RBF), (v) artificial neural networks (ANN), (vi) support vector regression (SVR), and (vii) hybrid response surface (e.g., AHF). The QRSM and AHF methods are adopted in this paper.

2.4.1. Adaptive hybrid functions (AHF)

The AHF methodology was developed by Zhang et al. [15] and has been shown to be a robust response surface technique. The AHF formulates a trust region based on the density of available training points, and it adaptively combines characteristically differing surrogate models. The weight of each contributing surrogate model is represented as a function of the input domain, based on a local *measure of accuracy* for that surrogate model. Such an approach exploits the advantages of each component surrogate, thereby capturing both the global and local trend of complex functional relationships. In this paper, the AHF integrates three component surrogate models—(i) RBF, (ii) E-RBF, and (iii) Kriging—by characterizing and evaluating the local *measure of accuracy* of each model. The detailed formulation of the AHF method can be found in the paper by Zhang et al. [15,33].

2.4.2. Quadratic response surface method (QRSM)

Although the AHF model presents high accuracy, the many numerical coefficients (of the response surface) and the complexity would restrict the usefulness of the WPP metric. Thus, the QRSM is also used for the WPP development, which involves fewer coefficients. The classical QRSM is one of the most widely used forms of response surface models in engineering design. A typical QRSM can be represented as

$$\tilde{f}_{qrsm}(x) = a_0 + \sum_{i=1}^{n_d} b_i x_i + \sum_{i=1}^{n_d} c_{ii} x_i^2 + 2\sum_{i=1}^{n_d-1}\sum_{j>i}^{n_d} c_{ij} x_i x_j \tag{11}$$

where the x_is are the input parameters; and the generic variables a_0, b_i, and c_{ij} are the unknown coefficients determined by the least squares approach.

2.4.3. Performance criteria

The overall performance of the response surface is evaluated using root mean square error (RMSE), which provides a global error measure over the entire design domain. The RMSE is given by

$$RMSE = \sqrt{\frac{1}{n_t}\sum_{k=1}^{n_t}\left(f(x^k) - \tilde{f}(x^k)\right)^2} \tag{12}$$

where $f(x^k)$ represents the actual function value for the test point x^k, $\tilde{f}(x^k)$ is the corresponding estimated function value, and n_t is the number of test points chosen for evaluating the error measure.

In addition, a cross-validation technique is used to ensure that the developed response surface is robust and accurate. The q-fold strategy (adopted in this paper) involves (*i*) splitting the data randomly into q roughly equal subsets, (*ii*) removing each of these subsets in turn, and (*iii*) fitting the model to the remaining $q-1$ subsets. If a mapping $\zeta : 1, \ldots, n \to 1, \ldots, q$ describes the allocation of the n training points to one of the q subsets and $\hat{f}^{-\zeta(i)}(x)$ of the predictor obtained by removing the subset $\zeta(i)$ (i.e. the subset to which observation i belongs), the cross-validation measure, prediction sum of squares (PRESS), is given by

$$PRESS_{SE} = \frac{1}{n}\sum_{i=1}^{n}\left[y^{(i)} - \hat{f}^{-\zeta(i)}(x^{(i)})\right]^2 \tag{13}$$

Hastie et al. [34] recommend compromise values of $q = 5$ or $q = 10$. In practical terms, using fewer subsets has an added advantage of reducing the computational cost of the cross-validation process by reducing the number of models that have to be fitted.

3. Numerical examples

In this paper, we explore two scenarios in the WPP evaluation. We consider a fixed-size (land) rectangular wind farm that consists of a defined turbine type. Two scenarios are considered here, given as

- Case 1: Evaluating the WPP (maximum capacity factor) of a farm that consists of 4 turbines;
- Case 2: Evaluating the WPP (maximum capacity factor) of a farm that consists of 9 turbines.

Both of the cases present $2N$ design variables. The GE 1.5-MW-XLE [35] turbine is chosen as the specified turbine type in both Case 1 and Case 2. The features of this turbine are provided in Table 1.

The specified wind farm properties are given in Table 2. The farm is oriented such that the positive X-direction of the layout coordinate system points toward the South. The rectangular farm size/orientation corresponds to an array configuration, with a row-wise spacing of seven times the turbine rotor diameter and a column-wise spacing of three times the turbine rotor diameter.

3.1. Response surface development

3.1.1. The AHF response surface

Case 1 investigates the wind potential by evaluating the maximum capacity factor of a wind farm with 4 turbines for a particular distribution of wind velocity at the site. For the 100 differing wind velocity distributions generated in SubSection 2.2, we obtain the

Table 1
Features of the GE 1.5-MW-XLE turbine [35].

Turbine feature	Value
Rated power (P_{r0})	1.5 MW
Rated wind speed (U_{r0})	11.5 m/s
Cut-in wind speed (U_{in0})	3.5 m/s
Cut-out wind speed (U_{out0})	20.0 m/s
Rotor diameter (D_0)	82.5 m
Hub height (H_0)	80.0 m

Table 2
Specified wind farm properties.

Farm property	Value
Land size (length × breadth)	Case 1: $7D_0 \times 3D_0$ Case 2: $(2 \times 7D_0) \times (2 \times 3D_0)$
Orientation	North to South lengthwise
Average roughness	0.1 m (grassland)
Density of air	1.2 kg/m^3

maximum capacity factor through UWFLO. These 100 sets of points are treated as the training points for the development of the response surface.

A cross-validation technique is used to evaluate the performance of the response surface (AHF) for various numbers of subsets. Fig. 3 shows the comparison of $PRESS_{SE}$ values to illustrate the accuracy of the response surface model. It is shown that, for the 4-turbine farm, the maximum values of $PRESS_{SE}$ are 0.0816 and 0.0013 for the bivariate normal and anisotropic lognormal distributions, respectively. The small $PRESS_{SE}$ values indicate a high accuracy of the estimated maximum capacity factor and the WPP. It is also observed from Fig. 3a that the estimation accuracy of the 4-turbine farm is generally better than that of the 9-turbine farm, with the exception of the 50 subsets cross-validation.

Case 2 investigates the wind potential by evaluating the maximum capacity factor of a farm with 9 turbines. We can see that, for the 9-turbine farm, the maximum values of $RPESS_{SE}$ are 0.0951 and 0.0019 for the bivariate normal and anisotropic lognormal distributions, respectively. Fig. 3b shows that, with the anisotropic lognormal distribution, the estimation accuracy of the 4-turbine farm is generally better than that of the 9-turbine farm, with the exception of the 10 subsets cross-validation.

The maximum capacity factor of distribution parameter combinations (4-turbine farm) are illustrated in Figs. 4a and b, where each diagram involves two parameters for ease of illustration. The 9-turbine farm case study is illustrated in Fig. 5. It is observed that the farm capacity factor increases with the mean wind speed. However, the capacity factor starts decreasing when the mean wind speed approaches 10.0 m/s. The observation can be attributed to the effect of the cut-out wind speed of the concerned turbine. The cut-out wind speed of the GE 1.5-MW-XLE turbine is 20.0 m/s at the hub height (80.0 m), which is equivalent to 10.2 m/s at the recorded data height of 3.0 m (the height at which the wind distribution is estimated), according to the log profile. In addition, we observe that the capacity factor is higher with a smaller value of wind direction standard deviation (Figs. 4a and 5a).

Figs. 4b and 5b show the maximum capacity factor of the combination of the (i) mean of the speed and (ii) standard deviation of the speed. It is observed that: (i) when the mean of the speed is larger, i.e. $\mu_u = 7.0$ m/s, the capacity factor increases while the standard deviation of the speed decreases; and (ii) when the mean of the speed is smaller, i.e. $\mu_u = 1.5$ m/s, the capacity factor has the maximum at the point $\sigma_u = 2.6$ m/s (approx.) and stops increasing when the standard deviation continues decreasing. This is because more high-speed winds are available with "small mean and large standard deviation values" compared to those with "small mean and small standard deviation values".

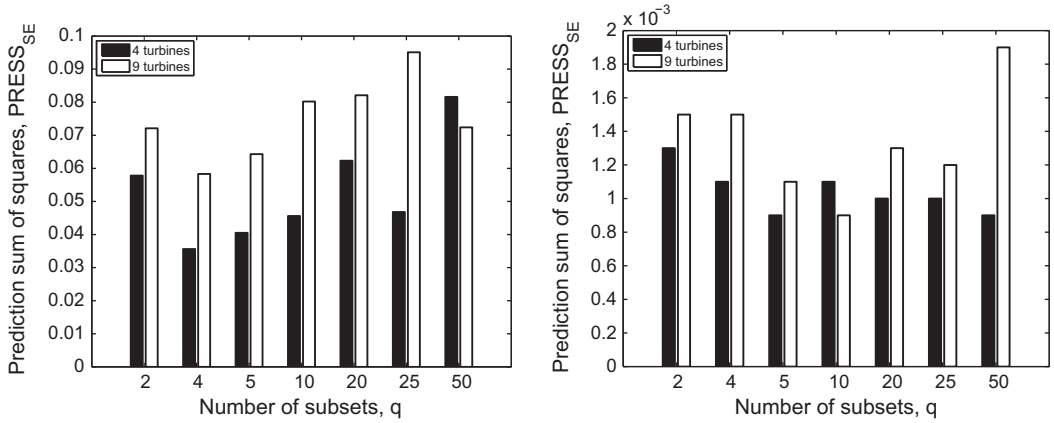

(a) Bivariate normal distribution (b) Anisotropic lognormal distribution

Fig. 3. Prediction sum of squares using the AHF response surface.

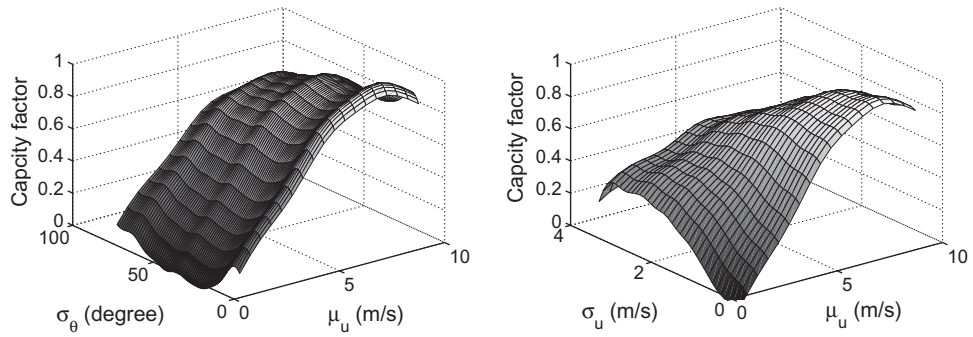

(a) Mean speed and direction standard deviation (b) Mean and standard deviation of speed

Fig. 4. Wind farm capacity of the bivariate normal distribution parameter combinations using the AHF response surface (4 turbines).

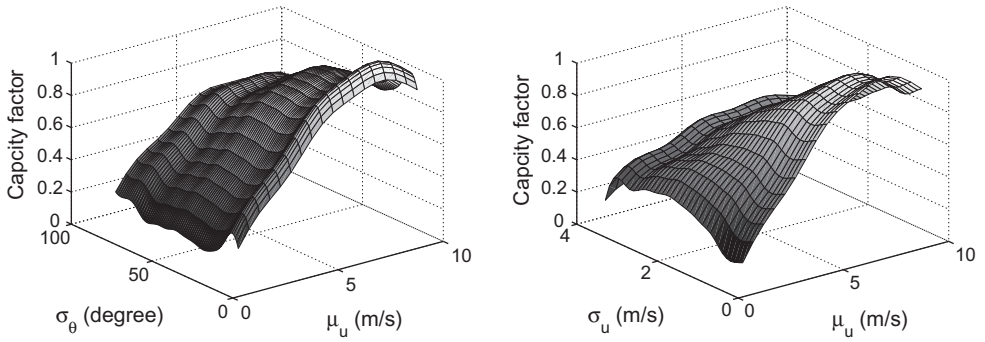

(a) Mean speed and direction standard deviation (b) Mean and standard deviation of speed

Fig. 5. Wind farm capacity of the bivariate normal distribution parameter combinations using the AHF response surface (9 turbines).

3.1.2. The quadratic response surface

Quadratic response surfaces are also developed for Case 1 and Case 2. The estimated values of the QRSM coefficients are listed in Table A.1. Figs. 6 and 7 show the maximum capacity factor of distribution parameter combinations. Similar trends with AHF estimations are observed from Figs. 6a and 7a. However, the trend illustrated by Figs. 6b and 7b is somewhat different than that shown in Figs. 4b and 5b. The observation can be attributed to the accuracy of the QRSM. QRSM formulates a smooth function with fewer coefficients, which is preferable in many engineering design problems. However, QRSM is often not adequate for capturing local accuracy in the close neighborhood of the training points.

3.2. Wind power potential (WPP) evaluation

For any farm site, according to the recorded wind data, we can estimate the parameters of the joint distribution of wind speed and direction (bivariate normal or anisotropic lognormal). Subsequently, we can predict the maximum capacity factor for the specified farm size and capacity using the WPP model. Four locations are selected to evaluate their wind power potentials. The wind data for these four locations is obtained from the North Dakota Agricultural Weather Network (NDAWN) [36]. The daily averaged data (wind speed and wind direction) in 2010 is measured and recorded at four differing stations (Ada, Baker, Beach, and Bottineau). Table 3 shows the latitude and longitude of the

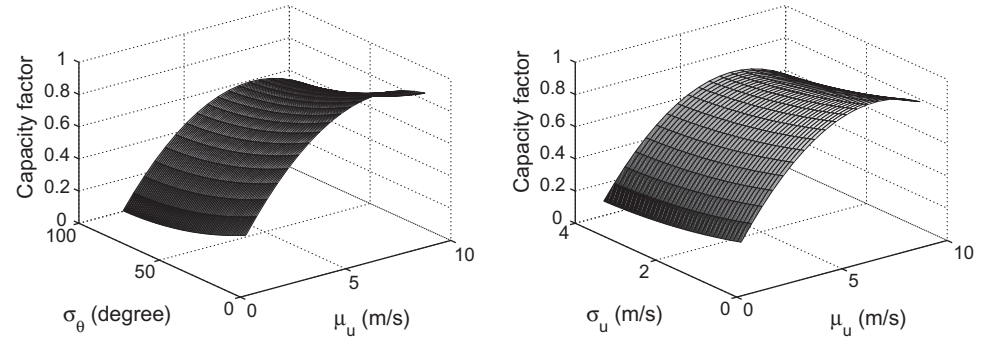

(a) Means peed and direction standard deviation (b) Mean and standard deviation of speed

Fig. 6. Wind farm capacity of the bivariate normal distribution parameter combinations using QRSM (4 turbines).

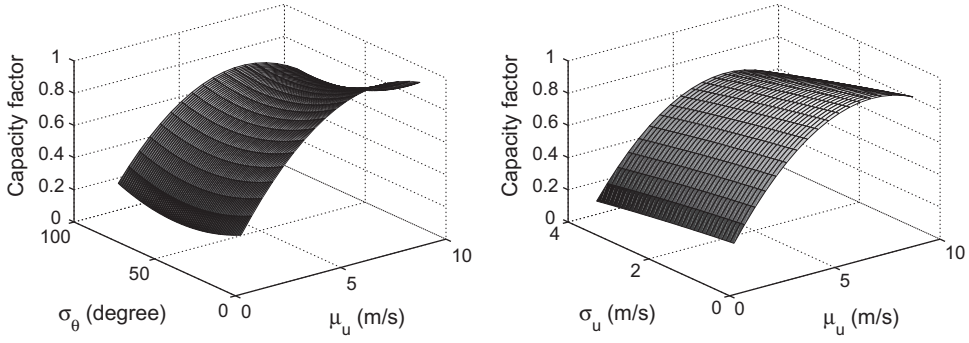

(a) Mean speed and direction standard deviation (b) Mean and standard deviation of speed

Fig. 7. Wind farm capacity of the bivariate normal distribution parameter combinations using QRSM (9 turbines).

stations. The parameters of the bivariate normal distribution for the four stations are estimated using maximum likelihood estimators, which are listed in Table 4. The parameters of the anisotropic lognormal distribution for the four stations are listed in Table 5.

The WPP is represented in terms of capacity factor (η), which is expressed as

$$\eta = \frac{OPG}{FRP} \tag{14}$$

where OPG represents the optimum power generation which is the maximum power generated by a wind farm with optimal layout; and FRP represents the farm rated power which is the installed capacity of a wind farm.

The WPP and capacity factor reference values are shown in Table 6. The RMSE value evaluated using Eq. (12) is 0.0053 for the 4-turbine farm and 0.0070 for the 9-turbine farm. The reference values of capacity factors are evaluated by the UWFLO framework using a multivariate and multimodal wind distribution (MMWD) model. The MMWD model, a wind distribution model to characterize the joint distribution of wind speed and direction, has been shown to be more accurate than most wind distribution models [21]. Both the WPP and UWFLO reference values show that Baker station is the best site for a wind farm. Wind rose diagrams at the four stations are illustrated in Fig. 8.

Table 3
Details of NDAWN station [36].

Station	Ada, MN	Baker, ND	Beach, ND	Bottineau, ND
Latitude	47.321°	48.167°	46.789°	48.821°
Longitude	−96.514°	−99.648°	−103.966°	−100.760°

3.3. WPP and WPD comparisons

Table 7 shows the siting ranking based on differing wind resource measures and UWFLO reference values. The numbers "1" and "4" represent the best and worst locations for wind farm sites among the four stations, respectively. The four sites are ranked based on the capacity factor values reported earlier in Table 6. WPD values at the measured height of the Ada, Baker, Beach and Bottineau sites are estimated to be 68.10 W/m^2, 69.20 W/m^2, 58.04 W/m^2 and 64.96 W/m^2, respectively. Both WPD and WPP (with a 4-turbine farm and 9-turbine farm) indicate that the Baker station is the best wind farm site. However, the WPD shows that the Beach station is the worst wind farm site, and the WPPs (with a 9-turbine farm) indicate different results. It is observed from the 4-turbine farm that: (i) the WPPs also show that the Beach station is the worst among the four stations for both bivariate normal and anisotropic lognormal distributions, which is the same as the result from the UWFLO reference; and (ii) the ranking of the WPP with a bivariate normal distribution is identical to that of the capacity factor evaluated by the UWFLO. For the 9-turbine farm, we observe that the (i) Ada station is the worst with a bivariate normal distribution; (ii) Bottineau station is the worst with an anisotropic lognormal distribution; and (iii) WPP with a bivariate normal distribution and the UWFLO reference indicate the same best and worst stations for a wind farm. The different rankings between 4-turbine and 9-turbine farms can be partially attributed to the wake effects in the farm. The wake of the 9-turbine farm is more complicated than that of the 4-turbine farm. Overall, the site ranking based on WPP is more accurate than that based on WPD. The wind resource measures (WPD and WPP) are normalized based on the WPD and WPP values at the Ada station, which are shown in Fig. 9. As shown, the WPD and WPPs follow different trends. In addition, we observe that the difference between WPP and WPD when using a bivariate normal distribution is more than that when using an anisotropic distribution.

Table 4
Bivariate normal distribution parameters estimated for the four stations.

Station	Mean speed, μ_U	Mean direction, μ_θ	Standard deviation of speed, σ_U	Standard deviation of direction, σ_θ	Correlation coefficient, ρ
Ada	3.89	197.45	1.89	101.04	0.10
Baker	3.94	195.51	1.83	103.74	0.07
Beach	4.00	219.24	1.44	85.97	0.13
Bottineau	3.91	196.38	1.78	103.49	0.15

Table 5
Anisotropic lognormal distribution parameters estimated for the four stations.

Station	Mean (lateral), $\mu_{x'}$	Mean (longitudinal), $\mu_{y'}$	Standard deviation (lateral), $\sigma_{x'}$	Standard deviation (longitudinal), $\sigma_{y'}$	Principle direction, θ_D (degree)
Ada	0.11	0.23	2.69	3.38	186.09
Baker	0.11	0.54	2.89	3.20	282.96
Beach	0.20	1.01	3.30	2.48	244.80
Bottineau	−0.09	−0.06	2.86	3.21	96.00

Table 6
Estimated capacity factors, η.

Station	WPP (4-turbine)		UWFLO (4-turbine) MMWD	WPP (9-turbine)		UWFLO (9-turbine) MMWD
	Bivariate normal	Anisotropic lognormal		Bivariate normal	Anisotropic lognormal	
Ada	0.4188	0.2586	0.3944	0.4852	0.2434	0.4429
Baker	0.4240	0.2794	0.4474	0.4957	0.2845	0.5250
Beach	0.4169	0.2164	0.3885	0.4929	0.2254	0.4589
Bottineau	0.4234	0.2264	0.4086	0.4910	0.2250	0.4597

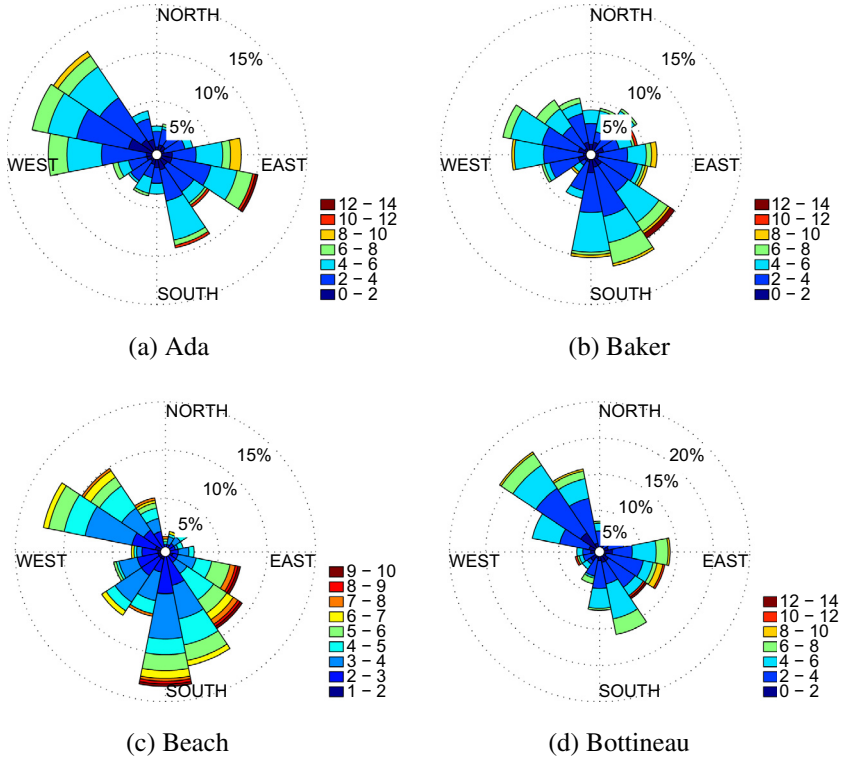

Fig. 8. Wind rose diagrams at four stations.

Table 7
Site ranking based on wind resource measures.

Station	WPP (4-turbine farm)		UWFLO	WPP (9-turbine farm)		UWFLO	WPD
	Bivariate normal	Anisotropic lognormal	(4-turbine) MMWD	Bivariate normal	Anisotropic lognormal	(4-turbine) MMWD	
Ada	3	2	3	4	2	4	2
Baker	1	1	1	1	1	1	1
Beach	4	4	4	2	3	3	4
Bottineau	2	3	2	3	4	2	3

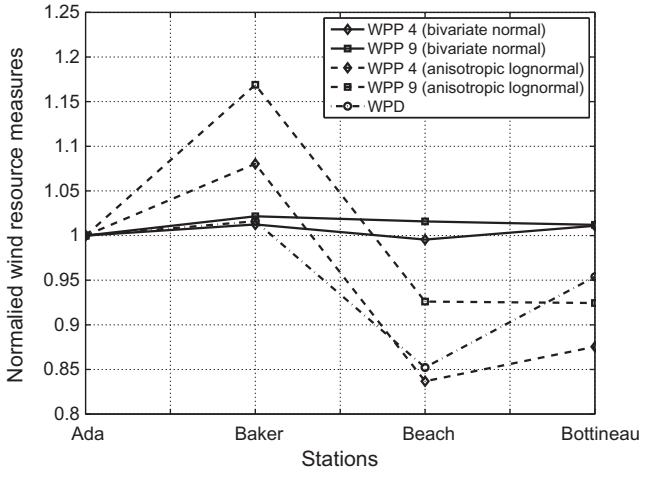

Fig. 9. Normalized wind resource measures at each station.

Table A.1
Coefficients of the QRSM model.

Coefficient	Bivariate normal		Anisotropic lognormal	
	4 turbines	9 turbines	4 turbines	9 turbines
a_0	0.2203	0.2367	0.1725	−0.2732
b_1	2.8163	2.8363	0.3097	0.4976
b_2	0.1543	0.2112	0.2423	0.4683
b_3	−0.3145	−0.1664	0.1136	0.0896
b_4	−0.3712	−0.3021	0.1094	0.2140
b_5	0.3707	0.1365	0.0564	0.1738
c_{11}	−2.9704	−2.9035	−0.2311	−0.3922
c_{22}	−0.5412	−0.5610	−0.2021	−0.3719
c_{33}	0.1107	−0.0255	−0.0234	0.0608
c_{44}	0.1910	0.3630	−0.0019	−0.0906
c_{55}	−0.2376	−0.0231	0.1065	0.0788
c_{12}	0.3394	0.4990	0.0258	0.0004
c_{13}	−0.1274	−0.1947	−0.0817	−0.0851
c_{14}	−0.1407	−0.3852	−0.0676	−0.0709
c_{15}	−0.1756	−0.0527	0.0066	−0.0357
c_{23}	0.2806	0.2535	−0.0318	−0.0616
c_{24}	0.2243	−0.0239	−0.0396	−0.0677
c_{25}	−0.1240	−0.0240	0.0078	−0.0155
c_{34}	0.0001	−0.0194	0.0519	0.0211
c_{35}	0.1272	0.1348	−0.1444	−0.2432
c_{45}	−0.1394	−0.2647	−0.1332	−0.1248

4. Conclusion

This paper developed a new wind resource potential measure: wind power potential (WPP), which would help decision makers in wind farm siting and design. This comprehensive measure characterizes and predicts the quality of wind resources by considering the joint distribution of wind speed and wind direction. The wind distribution was modeled using two differing methods: bivariate normal and anisotropic lognormal distributions. The farm capacity factor was maximized through layout design using the UWFLO methodology. Response surfaces were then constructed, using the AHF and QRSM, to represent the capacity factor as a function of the parameters of the wind distribution.

It was observed that: (i) the farm capacity factor increases with the mean wind speed, and starts decreasing when the mean wind speed approaches 10.0 m/s (measured at 3 m height); (ii) the capacity factor is higher with a smaller value of wind direction standard deviation; (iii) when the mean of the speed is larger, the capacity factor increases while the standard deviation of the speed decreases; and (iv) when the mean of the speed is smaller, the capacity factor has the maximum at the point $\sigma_u = 2.6$ m/s (approx.) and stops increasing when the standard deviation continues decreasing.

A comparison of four sites in North Dakota showed that WPD and WPP follow different trends. The ranking of candidate sites in terms of a realistic resource potential measure is not captured by WPD. The case study illustrated the variation of wind conditions and subsequently its influence on the quality of wind resources.

There are a few important considerations that one should be aware of when using the WPP metric. First of all, the WPP metric is subject to the assumptions made in the underlying models used to develop the metric. For example, (i) standard low fidelity analytical wake models are used to quantify wake losses in the context of estimating the wind farm energy production; (ii) a tractable bivariate unimodal normal distribution (with a small set of parameters) is used to represent the joint distribution of wind speed and direction, instead of using more complex models [21] that often involve a large number of parameters; and (iii) the analytical wind energy production models used in WPP are mostly applicable to a flat terrain. These assumptions are made to allow a tractable and computationally-efficient response surface, which is essential if the response surface is meant to serve as a guiding wind power potential metric for either comparing a large number of candidate sites or for developing wind resource maps – in such cases the overall relative trend of WPP is expected to hold in practice. However, in later stages of wind farm design, one is recommended to use higher fidelity (computationally complex and expensive) models to further analyze and optimize the wind farm(s) to be constructed.

In addition, special care should be taken when using WPP to compare sites that are (i) on complex terrain, (ii) known to experience multimodal wind distributions, or (iii) known to experience unique atmospheric boundary layer (ABL) phenomena (e.g., very high thermal stratification). Multi-fidelity models (e.g., combining large eddy simulation model with analytical wake models), i.e., models that offer attractive trade-offs between fidelity, computational cost, and tractability, are still in a nascent stage of development, especially in the context of wind energy applications. When such multi-fidelity models become more capable in the area of ABL and wind energy modeling, the WPP metric could then be trained using such multi-fidelity models to yield a more accurate and universally applicable metric for gauging the potential of wind farm sites.

Acknowledgements

Support from the National Science Foundation Award CMMI-1100948 is gratefully acknowledged. Any opinions, findings, conclusions, or recommendations expressed in this paper are those of the authors and do not necessarily reflect the views of the NSF. This work was also supported by the U.S. Department of Energy under Contract No. DE-AC36-08-GO28308 with the National Renewable Energy Laboratory.

Appendix A

Table A.1.

References

[1] Jamil M, Parsa S, Majidi M. Wind power statistics and an evaluation of wind energy density. Renew Energy 1995;6(5–6):623–8.
[2] Landberg L, Myllerup L, Rathmann O, Petersen EL, Jørgensen BH, Badger J, et al. Wind resource estimation – an overview. Wind Energy 2003;26:261–71.
[3] Celik AN. A statistical analysis of wind power density based on the Weibull and Rayleigh models at the southern region of turkey. Renew Energy 2003;9:593–604.
[4] Celik AN. Assessing the suitability of wind speed probability distribution functions based on wind power density. Renew Energy 2003;28(10):1563–74.
[5] Velo R, López P, Maseda F. Wind speed estimation using multilayer perception. Energy Convers Manage 2014;81:1–9.
[6] Lu L, Yang H, Burnett J. Investigation on wind power potential on Hong Kong islands – an analysis of wind power and wind turbine characteristics. Renew Energy 2002;27:1–12.
[7] Karsli VM, Geçit C. An investigation on wind power potential of Nurdagı-Gaziantep, Turkey. Renew Energy 2003;28:823–30.
[8] Rehman S. Wind energy resources assessment for Yanbo, Saudi Arabia. Energy Convers Manage 2004;45:2019–32.
[9] Boudia SM, Benmansour A, Ghellai N, Benmedjahed M, Hellal MAT. Temporal assessment of wind energy resource at four locations in algerian sahara. Energy Convers Manage 2013;76:654–64.
[10] Tizpar A, Satkin M, Roshan MB, Armoudli Y. Wind resource assessment and wind power potential of mil-e Nader region in Sistan and Baluchestan Province, Iran – part 1: Annual energy estimation. Energy Convers Manage 2014;79:273–80.
[11] Adaramola MS, Agelin-Chaab M, Paul SS. Assessment of wind power generation along the coast of ghana. Energy Convers Manage 2014;77:61–9.
[12] Chowdhury S, Zhang J, Messac A, Castillo L. Unrestricted wind farm layout optimization (uwflo): investigating key factors influencing the maximum power generation. Renew Energy 2012;38(1):16–30.
[13] Abramowitz M, Stegun IA. Handbook of mathematical functions with formulas, graphs, and mathematical tables. Mineola, New York: Dover Publications; 1972.
[14] Sobol IM. Uniformly distributed sequences with an additional uniform property. USSR Comput Math Math Phys 1976;16(5):236–42.
[15] Zhang J, Chowdhury S, Messac A. An adaptive hybrid surrogate model. Struct Multidisc Optim 2012;46(2):223–38.
[16] Myers RH, Montgomery DC. Response surface methodology: process and product optimization using designed experiments. 2nd ed. New York: Wiley; 2002.
[17] Vega R. Wind directionality: a reliability-based approach. Ph.D. thesis, Wind Science and Engineering, Texas Tech University, Lubbock, TX; August 2008.
[18] Carta JA, Ramírez P, Bueno C. A joint probability density function of wind speed and direction for wind energy analysis. Energy Convers Manage 2008;49(6):1309–20.
[19] Erdem E, Shi J. Comparison of bivariate distribution construction approaches for analysing wind speed and direction data. Wind Energy 2011;14(1):27–41.
[20] Weber RO. Estimator for the standard deviation of wind direction based on the moments of the Cartesian components. J Appl Meteorol 1991;30:1341–53.
[21] Zhang J, Chowdhury S, Messac A, Castillo L. A multivariate and multimodal wind distribution model. Renew Energy 2013;51:436–47.
[22] Zhang J, Chowdhury S, Messac A, Castillo L. Multivariate and multimodal wind distribution model based on kernel density estimation. In: ASME 2011 5th international conference on energy sustainability. Washington, DC: ASME; 2011.
[23] Kusiak A, Zheng H. Optimization of wind turbine energy and power factor with an evolutionary computation algorithm. Renew Energy 2010;35(3):1324–32.
[24] Bratley P, Fox BL. Algorithm 659: implementing Sobol's quasirandom sequence generator. ACM Trans Math Softw 1988;14(1):88–100.
[25] Chowdhury S, Zhang J, Messac A, Castillo L. Optimizing the arrangement and the selection of turbines for wind farms subject to varying wind conditions. Renew Energy 2013;52:273–82.
[26] Frandsen S, Barthelmie R, Pryor S, Rathmann O, Larsen S, Hojstrup J, et al. Analytical modeling of wind speed deficit in large wind offshore wind farms. Wind Energy 2006;9(1–2):39–53.
[27] Katic I, Hojstrup J, Jensen NO. A simple model for cluster efficiency. In: Proceedings of European wind energy conference and exhibition, EWEA, Rome, Italy; 1986.

[28] Zhang J, Chowdhury S, Messac A, Castillo L. A response surface-based cost model for wind farm design. Energy Policy 2012;42:538–50.
[29] Chowdhury S, Tong W, Messac A, Zhang J. A mixed-discrete particle swarm optimization algorithm with explicit diversity-preservation. Struct Multidisc Optim 2013;47(3):367–88.
[30] Chowdhury S, Zhang J, Messac A. Avoiding premature convergence in a mixed-discrete particle swarm optimization (mdpso) algorithm. In: 53rd AIAA/ASME/ASCE/AHS/ASC structures, structural dynamics and materials conference, AIAA, Honolulu, Hawaii; 2012.
[31] Forrester AIJ, Keane AJ. Recent advances in surrogate-based optimization. Prog Aerospace Sci 2009;45(1–3):50–79.
[32] Queipo N, Haftka R, Shyy W, Goel T, Vaidyanathan R, Tucker P. Surrogate-based analysis and optimization. Prog Aerospace Sci 2005;41(1):1–28.
[33] Zhang J, Chowdhury S, Zhang J, Messac A, Castillo L. Adaptive hybrid surrogate modeling for complex systems. AIAA J 2013;51(3):643–56.
[34] Hastie T, Tibshirani R, Friedman J. The elements of statistical learning. New York: Springer; 2001.
[35] GE, GE energy 1.5MW wind turbine brochure, general electric. <http://www.gepower.com/> (accessed December 2010).
[36] NDSU, The north dakota agricultural weather network. <http://ndawn.ndsu.nodak.edu> (accessed January 2012).